JOURNAL OF AIRCRAFT
Vol. 32, No. 3, May–June 1995

Damage Tolerance Certification of a Fighter Horizontal Stabilizer

Jia-Yen Huang,* Ming-Yang Tsai,† Jong-Sheng Chen,* and Ching-Long Ong‡
Aeronautical Research Laboratory, Taichung, Taiwan, Republic of China

A review of the program for the damage tolerance certification test of a composite horizontal stabilizer (HS) of a fighter is presented. The object of this program is to certify that the fatigue life and damage tolerance strength of a damaged composite horizontal stabilizer meets the design requirements. According to the specification for damage tolerance certification, a test article should be subjected to two design lifetimes of flight-by-flight load spectra simulating the in-service fatigue loading condition for the aircraft. However, considering the effect of environmental change on the composite structure, one additional lifetime test was performed. In addition, to evaluate the possibilities for extending the service life of the structure, one more lifetime test was carried out with the spectrum increased by a factor of 1.4. To assess the feasibility and reliability of repair technology on a composite structure, two damaged areas were repaired after two lifetimes of damage tolerance test. On completion of four lifetimes of the damage tolerance test, the static residual strength was measured to check whether structural strength after repair met the requirements. Stiffness and static strength of the composite HS with and without damage were evaluated and compared.

Introduction

TO certify that the structure of a newly developed aircraft meets the design requirements, a series of structural tests should be performed, including static strength, ground vibration, damage tolerance, and flight test.[1] Basically, these tests not only provide data for optimum design of aircraft, but also ensure the structural safety. During the last decade, laminated composites, with their high strength-to-weight ratio, offer considerable technological advances in the production of aircraft structures. However, the design is complex due to the nonhomogeneous nature of the material and its failure modes. Delaminations in the composite skins could result in stiffness and strength loss, thereby reducing the flutter resistance and strength margin of the structures. The general procedure for damage tolerance with respect to the development and verification of composite structures includes the following tasks: classification and determination of damage, determination of critical damage sizes and residual strength, damage tolerance tests, comparisons between test and analytical results, and the integration of all design criteria.[2] Seeing that no general rules of damage tolerance for composite structures are available, an individual procedure adapted to the structure to be developed has to be defined. In this article, the damage tolerance test of a composite horizontal stabilizer of a fighter is introduced and discussed thoroughly.

According to the specifications,[3,4] a test article must be able to sustain its structural integrity for two design lifetimes of a damage tolerance test to guarantee the safety of flight for one service lifetime. However, considering that the composite structure is sensitive to the change of environmental conditions, which is difficult to simulate in the test laboratory for a full-scale article, one additional lifetime of the test was performed to cover this effect.[2] During the damage tolerance test, strain surveys and nondestructive inspection (NDI) were carried out periodically to monitor strain distribution and to record damage growth. Since no apparent fatigue damage growth was found after three lifetimes of damage tolerance test, one more lifetime of the test with its load spectrum increased by a factor of 1.4 was carried out to evaluate the possibilities for extending the service life of the structure. Consequently, the test article has been subjected to four lifetimes of flight-by-flight load spectra simulating the in-service fatigue loading condition for the aircraft.

To certify the feasibility and reliability of repair technology on composite structures, two impact damaged areas were repaired after two lifetimes of a damage tolerance test. Both flush composite bonded repair and metal bolted repair were applied to the composite lower skin. Finally, on completion of four lifetimes of a damage tolerance test, a static residual strength test was performed to check whether structural strength after repair implementation met the requirements. Stiffness and static strength of the composite horizontal stabilizer (HS) with and without damage were evaluated and compared.

Structural Description

The composite horizontal stabilizer includes the following structural elements: 1) composite upper and lower skins, 2) composite sine wave corrugated substructure, 3) metallic leading edge and trailing edge, and 4) metallic tip rib and root rib. These are shown schematically in Fig. 1. The upper and lower composite skins were made of Fiberite T300/976 graphite/epoxy prepreg with material properties given as follows:

$$E_{11} = 138 \text{ GPa}$$

$$E_{22} = E_{33} = 8.8 \text{ GPa}$$

$$G_{12} = G_{13} = G_{23} = 4.5 \text{ GPa}$$

$$\nu_{12} = \nu_{13} = \nu_{23} = 0.3$$

The skins were symmetric to each other and were designed as quasi-isotropic stacking sequence with 0, 45, 90, and −45 deg in about equal proportions. The zero direction of fiber was arranged along the spanwise direction of spar line six. The laminate thickness varies from 16 plies near the tip of the HS to 64 plies near the region of the pivot shaft. In contrast

Received Nov. 29, 1993; revision received Nov. 1, 1994; accepted for publication Nov. 15, 1994.

*Associate Scientist, Aero Industry Development Center, P.O. Box 90008-11-3.

†Assistant Scientist, Aero Industry Development Center, P.O. Box 90008-11-3.

‡Senior Scientist, Aero Industry Development Center, P.O. Box 90008-11-3.

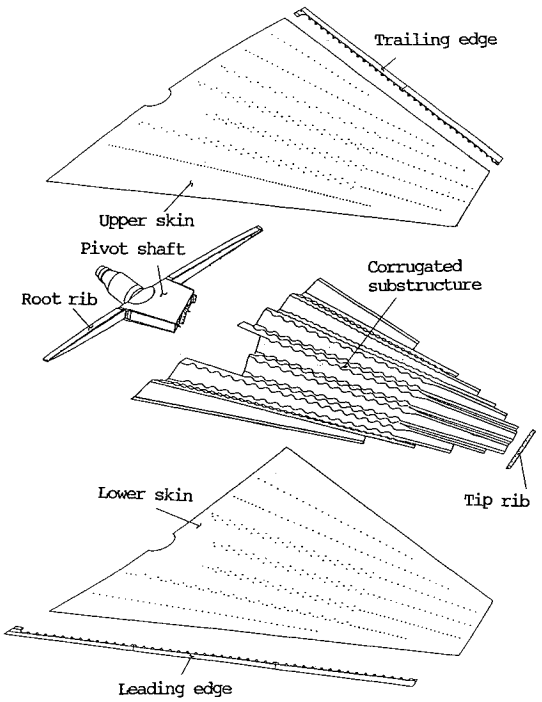

Fig. 1 Composite horizontal stabilizer components.

to a plane plate, the stability of the corrugated plate was influenced by many parameters that had been investigated,[2] including the angle of corrugation, radius of corrugation, overall plate dimension, and thickness of the laminate. Even though the cost of composite corrugation is high, the laminate thickness can be reduced without sacrificing the buckling strength. Thus, the aim of weight saving was attained. The horizontal stabilizer is classified as a safety-of-flight structure. Skins, corrugated substructure, and metallic pivot shaft are assembled with bolts and rivets.

Pretests for Test Parameters Evaluation

The damage tolerance tests are influenced by numerous factors; e.g., test procedures and boundary conditions of the test article. To get a realistic result for the structural capacity with respect to damage tolerance, these factors have to be clarified and defined. The impact damage tolerance test was proceeded by tests of components (panels) to get the test parameters. The completion and review of these parameters was done by a test of the substructure, the bending-torsion (BT) box,[2] to reach the realistic test procedure to be performed in the damage tolerance test.

To get realistic information on the damage tolerance data for the HS, attention has to be paid to the impact test parameters on specimens or components, including impact energy, type of impactor, geometry, support conditions, material properties, specimen thickness, stacking sequence, and loads. The purpose of the impact pretests is to verify the input parameters of testing the HS under the realistic boundary conditions. The procedure and performance steps are as follows. First is the selection of the critical areas of the HS. Second is the definition of test point geometry and support conditions. Third is the definition of the test parameters such as impact energies and impactor size and form. Usually, the impactor size and form are determined by considering the real impact conditions during manufacture and service. Finally, test results evaluation, i.e., damage size measurement by A-scan as a function of the impactor type and energy. The results of the impact pretests defined the reference data for the damage tolerance tests of the HS.

The finite element analyses with its model shown in Fig. 2 have been carried out for evaluating load distribution of the

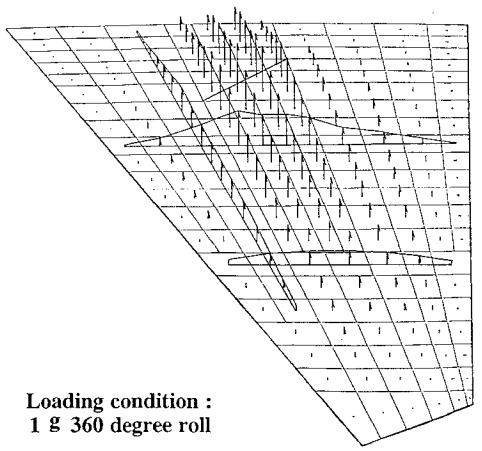

Fig. 2 Finite element model and normal force distribution for evaluation of the critical load case.

critical load case. The normal force distribution was evaluated from a 1-*g* 360-deg roll with a speed of Mach number 1.8 and an altitude of 6400 m. The objective of the analysis is to provide the correct internal forces and load path for selection of impact locations. Since complex load paths are prone to fracture, especially the places with stress concentration, these regions are the candidate points for impact test.

Damages Simulation

Because the metallic pivot shaft had already been proved to meet design requirements, in this article focus is on the damage tolerance certification of composite parts, including skins and corrugated substructure. In general, graphite–epoxy composites have the advantage of resistance to cracking by spectrum loading and immunity to corrosion. However, damage occurring during service may cause significant reductions in compressive strength. Of all the damage types that are possible during manufacture and service, delaminations, impact damages, lightning strike damage, battle damages, and loose rivets were selected for the damage tolerance test because of their important effects on structural capacity. Although an amount of delaminations may be induced by impact, only a slight indentation was observed. Unless the region is subjected to NDI, this type of damage, frequently referred to as barely visible impact damage, is unlikely to be discovered.[5] Since the artificial flaws of comparable area to impact damage produce less reduction in compressive strength,[5] and also considering the estimated expenditure, delaminations were simulated by serious impact damage only. The distribution of simulated damage on the lower and upper skins is shown in Figs. 3 and 4, respectively. There were 25 damaged locations, including 13 barely visible impact damage (BVID), 8 visible impact damage (VID), 1 lightning strike damage, 1 battle damage, and 2 loose rivets. Note that damage on the corrugation, four BVID and three VID, which were applied before the process of assembly with composite skins, have not been shown on Figs. 3 and 4. Considering that the delamination is prone to spread under compressive loading, most of the damage (14 locations) was applied to the lower skin.

The critical load case has to be decided together with the detailed damage locations. The load types can be expected to be the same as those for the BT box. The results of the impact pretest and parameters investigated by the BT box test defined the reference data for the damage tolerance tests of the HS. The selections of impactor and impact energy were based on BT box results, while the impactor form was based on panel test results.

The equipment for the impact test includes vertical guides for the impactor with small friction, a meter for measuring impact height, instruments for preventing secondary impact and for adjustment of impact position. The weight changeable

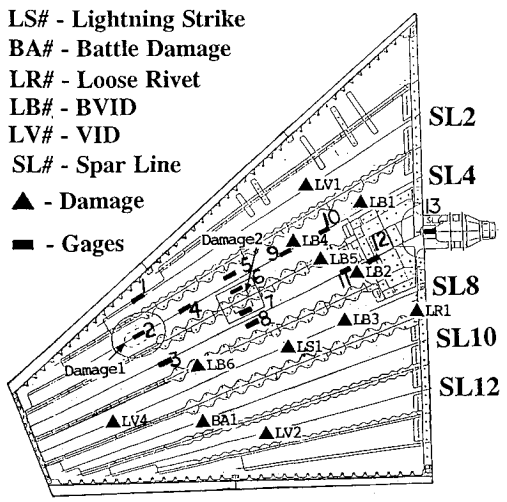

Fig. 3 Distribution of simulated damage and strain gauges on the lower skin.

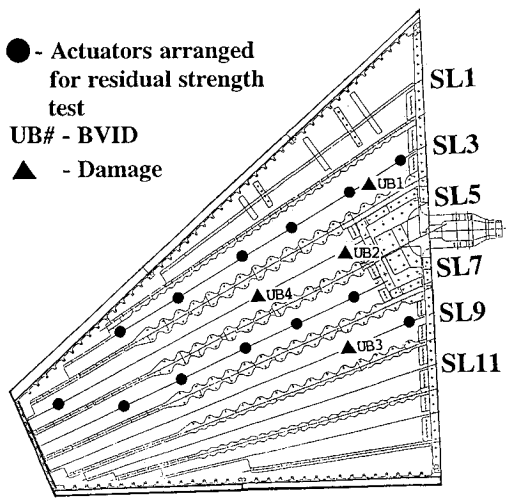

Fig. 4 Distribution of simulated damage and strain gauges on the upper skin.

impactor, with a 25.4-mm-diam steel dart head, is a drop weight. The impact energies, which can be controlled by adjusting the height and weight of the impactor,[6] are the products of height and weight of the impactor. The exact positions to be impacted, especially at the ply termination, can be identified by measuring the thickness of the laminate with the help of portable NDI (A-scan). In addition, any existing manufacturing defects around the impact positions must be detected. Again, NDI was utilized to determine the extent of the internal damage of the structure after impact. Since actual damage sizes may differ from the planned damage, the test was started with impacts in less critical areas.

Because the high resistivity of an unprotected composite does not allow the damaging energies of lightning to dissipate quickly, puncture or severe delamination of the skins[7] may result. An analysis had been made of the probable lightning strike zones of the fighter, guiding the design of lightning protection material. The skin near the tip of the HS is classified as a region of initial attachment point with low probability of flash hang-on.[4] Considering that the metallic tip rib can act as a good conductor for releasing the lightning energy, no severe lightning damage will be expected on the skins. On the whole, most areas of the HS are zones of low probability of lightning strike. Yet, for the sake of safety, oxidized damage on composite skin caused by lightning strike was simulated in the damage tolerance test by grinding four plies off with a tapered circular hole with 100 mm in diameter at the first ply and 50 mm in diameter at the fourth ply. As for the test of bolt failure effect on the structure capacity, damage from loose rivets was simulated by removing some blind bolts. Battle damage was simulated by drilling a hole on the composite skin.

Damage Tolerance Test

The detailed procedures of the HS damage tolerance test are 1) definition of the areas to be damaged and corresponding application of strain gauges; 2) reference test: static and undamaged; 3) impacting of the critical areas; 4) NDI for evaluating the damaged area; 5) performance of the structure test; 6) NDI between the different load-steps and types; 7) record of the test results: damage size, stiffness, strain distribution, and residual strength; and 8) disassembly of the HS and inspection for the damaged parts.

According to the specifications,[3,4] two design lifetimes of damage tolerance test should be performed. However, considering that the composite structure is sensitive to environmental change, which is difficult to simulate in the test laboratory for a full-scale article, the first lifetime damage tolerance test with BVID defects was carried out to assess environmental effects.[2] The composite HS exceedance curves, generated from the lifetime load spectrum, are shown in Fig. 5. For the following two lifetimes of test, visible impact damages, large delaminations, lightning strike, and loose rivets were applied to the HS to assess the damage tolerance characteristics. The impact test data for upper and lower skins are shown in Table 1. Finally, one lifetime testing with its magnitude of load increased to 140% was carried out to evaluate

Table 1 Impact test data for upper and lower skins

Impact damage	Thickness, mm	Impact energy, J	Damage area, mm^2
UB1	5.5	21.7	1050
UB2	8.5	39.4	3341
UB3	6.4	28.1	1280
UB4	6.3	26.5	1644
LB1	6.7	26.4	3330
LB2	8.5	24.0	2797
LB3	7.3	32.3	2035
LB4	6.5	22.1	1210
SL1	7.7	19.3	831
SL2	4.1	11.5	1300
LV1	4.4	14.9	888
LV2	3.2	9.9	884
LV3	3.1	15.2	4734
LV4	3.1	8.6	361
BA1	3.1	37.9	3392

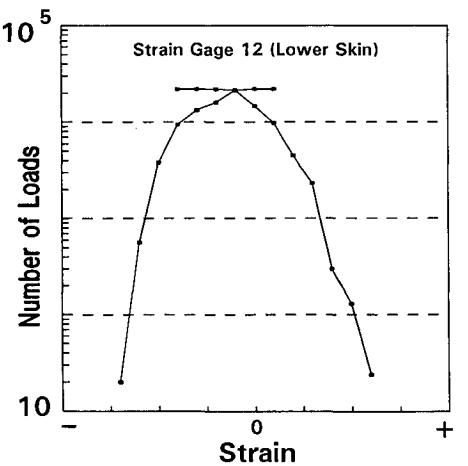

Fig. 5 Exceedance curves of fatigue test spectrum.

the possibilities for extending the service life of the HS. Totally, the test article was subjected to four lifetimes of flight-by-flight load spectra simulating the in-service fatigue loading condition for the aircraft.

Strain surveys and NDI inspections were taken periodically to track the strain history and damage growth as shown in Figs. 6 and 7, respectively. Generally speaking, lightning strike and loose rivets did not induce significant delamination growth. The stable strain history and low damage growth rate indicated that in-service spectrums with 2000 μ maximum strain have no significant effect on the damage of the composite HS. Even when the spectrum was increased to 140%, the same phenomenon was observed, damage extended a small amount at the beginning and eventually stopped growing. Since LB no. 4 is one of the most severely damaged and it is close to damage LB no. 5, it is likely that the damage may grow more rapidly due to interaction. However, that the size of damaged area of LB no. 4 stopped growing after 10,000 flight hours provided the evidence that the interaction effect between two damage sites can be neglected. By investigating the exceedance curves shown in Fig. 5, the lower skin was subjected to a compression dominant spectrum. Therefore, the growth rate of damage on the lower skin was expected to be more severe than that of the upper skin. However, the estimation was in contradiction to the results shown in Fig. 7. Because the loading system was applied on the upper skin, further tests are needed to check whether or not the fast-growing rate of upper skin was induced by an out-of-plane tension force from this loading system.

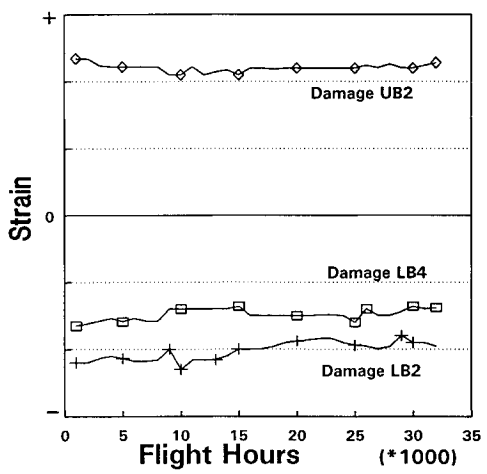

Fig. 6 Strain history of critical damage of lower and upper skins.

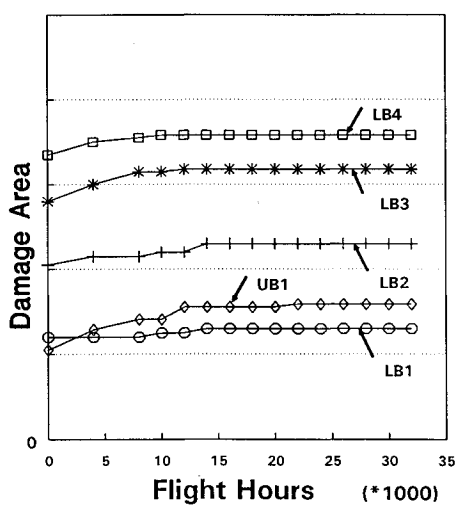

Fig. 7 Damage growth of critical damage of lower and upper skins.

Repair

Two kinds of repairs, flush composite patch repair shown in Fig. 8 and flush metal bolted repair shown in Fig. 9, were applied to the lower skin before the third lifetime damage tolerance test was performed. The object of repair is to restore the strength and stiffness of damaged structure up to the original. To minimize the influence of repairs on the characteristics of a structure, proper repairs have to be designed by considering many parameters such as stiffness, strength, surface smoothness, assembly, and sealant requirements. In general, external patches are much easier and faster to apply, but their efficiency is low.

The locations of two damaged areas with patch repairs are shown in Fig. 3. Damage 1 with its dimension 50.8 by 127 mm lies between spar 3 and spar 5; damage 2 with its dimension 101.6 by 127 mm is located at spar 5 in 5.6-mm-thick skin. For damage 1 located in 3-mm-thick skin, which is too thin for bolted repair,[8,9] the damaged region was removed along its elliptical shape revealed by NDI. To transfer the load smoothly between the undamaged and damaged region, minimizing the peak shear stresses and peel stresses in the adhesive layer, a tapered hole with 18:1 length-to-thickness ratio was ground, and a patch with the same tapered shape and the same stacking sequence as the skin was bonded. Over this region, a protective cover with three sawtoothed layers of prepreg was bonded to the parent laminate, shown in Fig. 8, to reduce the peel stress and shear stress along the edge of patch. For damage 2, covering the regions of spars 3, 5, and 7, is difficult for a flush-bonded patch, and so a flush metal bolted patch was applied. After cutting damage 2 into

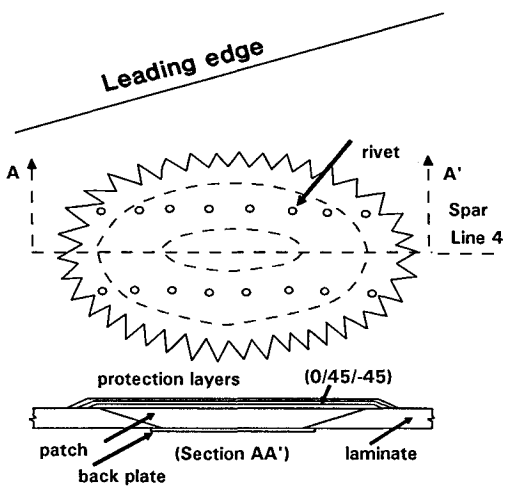

Fig. 8 Schematic showing the flush composite bonded repair.

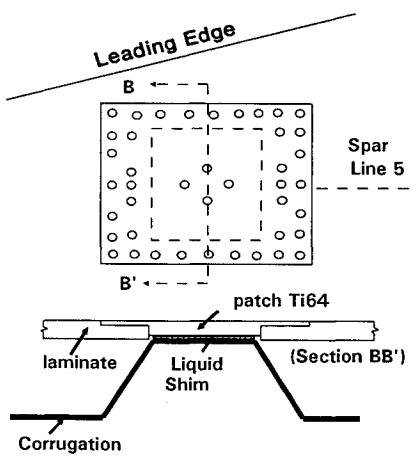

Fig. 9 Schematic showing the bolted titanium patch repair.

Table 2 Detail data for flush composite bonded repair

Damage size	Elliptical graphite/epoxy laminate 127 mm × 50.8 mm
Layup of damaged skin	$[0/45/0/-45/90/45/0/-45/0/45/90/-45]_s$, 24 layers
Modulus of damaged skin	$E_x = 55.8$ GPa $G_{xy} = 18$ GPa $E_y = 38.4$ GPa $\nu_{xy} = 0.381$
Patch size	Elliptical graphite/epoxy patch, 299.7 mm × 223.5 mm
Layup of patch	Same as the layup of damaged skin, 24 layers
Layup of protection layers	[0/45/−45], Three sawtoothed layers
Modulus of patch	$E_x = 55.7$ GPa $G_{xy} = 18.5$ GPa $E_y = 36.6$ GPa $\nu_{xy} = 0.41$

Table 3 Detail data for bolted titanium patch repair

Damage size	Rectangular 101.6 × 127 mm
Layup of damaged skin	$[(0/45/0/-45)_2/90/45/90/-45/-45/0/45/90/-45/0/45/45/90/-45]_s$, 44 layers
Modulus of damaged skin	$E_x = 49.7$ GPa $G_{xy} = 19.3$ GPa $E_y = 40.4$ GPa $\nu_{xy} = 0.383$
Patch size	Rectangular Ti64, 210.8 × 190.5 × 4.1 mm
Modulus of patch	$E_t = 110.3$ GPa $G = 42.7$ GPa $E_c = 113.1$ GPa $\nu = 0.31$

Table 4 Strain distribution around patches before and after repair implementation

Gauge number	Strain variation
1	——
2	−3.9%
3	−15.4%
4	——
5	+26.5%
6	——
7	——
8	−40.7%
9	+1.3%
10	——
11	−10.2%

Table 5 Comparisons of averaged strain of lower skin before and after the patches were employed

Gauges on lower skin	Strain comparison, averaged
Between spars 1 and 3	+4.8%
Between spars 5 and 7	−9.9%
Between spars 7 and 9	−3.9%
Between spars 9 and 11	−4.6%
Between spars 11 and 13	−6.0%

a square hole, a titanium plate shown in Fig. 9 was bolted to the skin and corrugate. Both patchs were designed by equivalent stiffness concept as

$$E_c t_c = E_p t_p \tag{1}$$

where the subscripts c and p denote composite laminate and patch, respectively. E is the equivalent Young's modulus; t is the thickness of laminate or patch. The equivalent stiffness of the composite patch, which can be calculated from the data shown in Table 2, was about 12% higher than that of skin.[10] The metallic patch, made of Ti64 alloy, has a higher stiffness and strength than composite skin, as shown in Table 3, with no severe galvanic corrosion when in contact with composite material. Table 4 shows the strain distribution around damaged regions subjected to the maximum spectrum loading condition before and after repair implementation. The strain at gauge 3, near the trailing edge of the bonded patch, was reduced 15.4%. The strain value forward of the bolted patch (gauge 5) increased 26.5%, while afterward of the patch (gauge 8) it decreased 40.7%. Although there were stress concentration effects around the patches, the strain history around the patches kept a stable value during the two lifetimes test. The strain distribution comparison of the whole structure with and without repairs is shown in Table 5, indicating that the repairs have no significant influence on the load path of the structure.

Residual Strength Test

Static strength tests of the composite HS, the final and most important test item, were aimed at investigating the influences of damages on structure stiffness and strength and also in proving the strength of repairs. To simulate a better design limit load condition, 13 load actuators, shown in Fig. 4, and

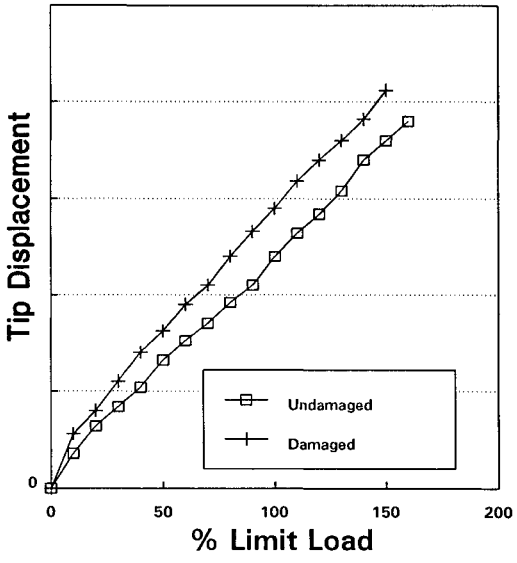

Fig. 10 Comparison of tip deflections between damaged and undamaged composite horizontal stabilizer.

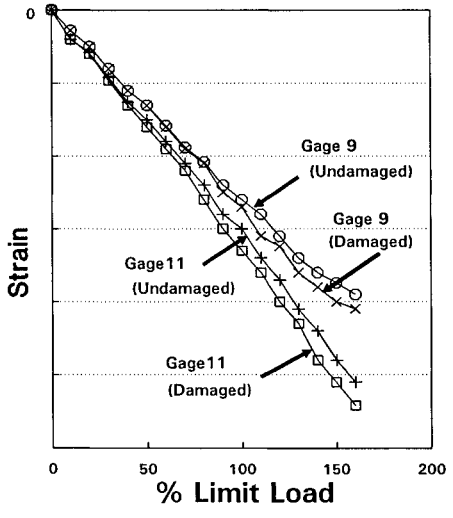

Fig. 11 Comparison of strain between damaged and undamaged composite horizontal stabilizer.

the offset concept that allows the actuators to adjust their loading direction were used. Nine potentiometers were arranged at different regions of structure to measure the displacements of the composite HS subjected to static load. When the bolts located in the middle of gauge 1 and the tip of HS failed, which subsequently caused the lower skin to buckle, the test was stopped.

For composite HS without damage, the static strength attains 175% design limit load. Tensile failure modes were found at the bolted region of upper skin and pivot fitting. For the composite HS with 23 damaged areas and two repairs, the residual static strength attains 160% limit load, which meets the regulation[2]: the damaged HS structure must be capable of sustaining limit load without any failure or obvious partial failure. Although, as shown in Fig. 10, the comparison of the tip displacement between damaged and undamaged composite HS indicates that the stiffness of the repaired structure is slightly lower than that of the undamaged structure, no significant difference of strain was found around critical areas of the HS as shown in Fig. 11. Note that the two repaired regions survived after being subjected to 160% limit load, hence, structure with damage of the tested sizes and locations is repairable. This test provides an important reference for service maintenance.

Conclusions

This article presents the structural certification of fatigue life and damage tolerance strength in developing the composite HS of a fighter. Test items include simulation of damage of composite structure, four lifetime test of flight-by-flight load spectra, bonded and bolted repairs of composite structure, and static residual strength test. Conclusions from these tests can be summarized as follows:

1) To get a realistic result for the structural capacity with respect to damage tolerance, the impact test should start with tests of components to clarify and define the test parameters. The completion and review of these parameters studied should be done by tests on substructure to determine the realistic test procedure to be performed in the damage tolerance test for the composite HS.

2) Damage to composite structure was more difficult to simulate than that of metallic structure. Of all the damage types that are possible during manufacture and service, impact damages, lightning strike damage, battle damages, and loose rivets should be applied to composite skins and corrugation for damage tolerance test. The environmental effect and the possibilities for extending the service life of the structure can be investigated by additional lifetime testing.

3) The design and processes for flush composite bonded and metallic bolted repair were proved feasible and reliable. These data provide essential reference for service maintenance of composite HS.

4) Due to the lack of a general handbook of damage tolerance for composite structures, an individual procedure adapted to the structure to be developed has to be defined. The damage tolerance certification procedure developed for the HS of a fighter can be applied to other composite structures as long as relevent data are provided.

References

[1]Chang, Y. B., Lin, T. Y., Wang, G. R., and Chen, C. C., "Flight Load Test of the Indigenous Defensive Fighter," *Journal of Aircraft*, Vol. 31, No. 4, 1994, pp. 946–952.

[2]Tsai, M. Y., "Test Plan for Damage Tolerance Test of Composite Horizontal Stabilizer," Aeronautical Research Lab., Aero Industry Development Center, RT-128, Taiwan, ROC, Jan. 1990.

[3]"Military Specification, Airplane Damage Tolerance Requirements," MIL-A-83444, U.S. Air Force, July 1974.

[4]"Military Specification, Airplane Strength and Rigidity Ground Tests," MIL-8867B, U.S. Air Force, Aug. 1975.

[5]Jones, R., and Baker, A. A., "Compressive Strength of Impact Damaged Graphite Epoxy Laminates," *Composite Structures*, Vol. 3, edited by I. H. Marshall, Elsevier, London, 1985, pp. 402–414.

[6]Joshi, S. P., and Sun, C. T., "Impact-Induced Fracture in a Quasi-Isotropic Laminate," *Journal of Composite Technology and Research*, Vol. 9, No. 2, 1987, pp. 40–46.

[7]Triplett, T. E., "Lightning Strike Protection Concepts for Composite Materials," *34th International SAMPE Symposium*, 1989, pp. 96–107.

[8]Labor, J. D., and Myhre, S. H., "Repair Guide for Large Area Composite Structure Repair," Air Force Flight Dynamics Lab. AFFDL-TR-79-3039, March 1979.

[9]Myhre, S. H., and Beck, C. E., "Repair Concepts for Advanced Composite Structures," *Journal of Aircraft*, Vol. 16, No. 10, 1979, pp. 720–728.

[10]Tsai, S. W., *Introduction to Composite Material*, Technomic, Westport, CT, 1980, pp. 121–166.